Bridge Maintenance, Safety, Management, Digitalization and Sustainability – Jensen, Frangopol & Schmidt (eds)

Retrofit of PRC bridges by external post-tension under different corrosion scenarios

G. Santarsiero, V. Picciano, A. Masi & G. Ventura
School of Engineering, University of Basilicata, Potenza, Italy

ABSTRACT: Prestressed reinforced concrete bridges with post-tensioned strands are subjected to heavy corrosion deterioration problems due to injection defects and chloride ingress by de-icing salts or sea airborne. The peculiarity of this prestressing system is recognized by the new italian guidelines on existing bridges prescribing special assessment procedures. Therefore, these bridges need reliable strengthening techniques able to enhance durability reducing the risk of collapse. This paper examines the application of post-tension to rehabilitate pc bridges with injected cables, considering corrosion initiation and propagation, estimated through a chloride ingress model included in the finite element models. Assuming a high chlorides surface concentration, a case study bridge is investigated to design an external post-tension intervention evaluating the time evolution of the capacity-demand ratio under gravity and traffic loads. The capacity loss is estimated depending on the considered corrosion period also assessing the response in terms of cracking and deformation.

1 INTRODUCTION

Following the Second World War, Italy witnessed a growing development of its infrastructure network, so much that it could compete with the main European cities. The majority of the bridges along the road networks were constructed during that period and, as a result, they are now in a state of obsolescence and degradation due to reaching the end of their design service life (Di Prisco 2019).

During those years, the most used technologies for bridge construction were reinforced concrete and prestressed reinforced concrete with post-tensioned cables, which presented significant issues related to degradation due to cable corrosion. In fact, due to the execution deficiencies of this technique, which was still in its early stages during those years, a widespread error was primarily associated with the incorrect or sometimes complete lack of grout injection into the ducts (Smith & Wood 2001), resulting in the creation of voids that facilitated chloride ingress due to the use of de-icing salts or marine aerosol, subsequently initiating and promoting tendon corrosion (Gjørv 2009).

Another critical aspect is that, for this type of structure, is difficult to detect ongoing corrosion phenomena through simple visual inspection or the most common non-destructive diagnostic techniques. Therefore, they may be in a significantly degraded condition not visible from the outside, which can lead to the sudden collapse of the structure (Godart 2015).

For these reasons, within the Italian code for existing bridges, namely the Guidelines on risk classification and management, safety assessment and monitoring of existing bridges (Ministry of Infrastructure, CSLP 2020), prestressed concrete bridges with post-tensioned cables are classified as structures that require accurate assessments and the implementation of special inspections, given their inherent vulnerability.

Therefore, an accurate assessment of safety levels and residual functionality is of fundamental importance, primarily for bridges that are clearly in a state of degradation, but also for bridges that, while appearing to be in optimal preservation conditions, may still exhibit obsolescence, even if only in terms of regulatory compliance, as they were designed according to the specifications of older technical standards (Santarsiero et al. 2023).

DOI: 10.1201/9781003483755-65

Following the safety assessments required by current regulations, most of the existing bridges and viaducts show an actual capacity lower than the demand generated by current traffic loads, which are significantly higher than those considered at the design time of each structure. Therefore, it is necessary to take action through strengthening measures to restore the lost load-bearing capacity due to current degradation conditions and/or the gap in terms of the capacity-demand ratio to satisfy safety verifications.

The purpose of this study is to evaluate the effectiveness of a rehabilitation intervention for existing bridges with a prestressed reinforced concrete girders deck, employing external post-tensioning cables. Specifically, using nonlinear numerical analyses conducted with the finite element software ATENA (Červenka et al. 2021), the overtime decay of the load-bearing capacity of the most stressed beam was first evaluated, considering different time scenarios of damage associated with the onset of chloride-induced corrosion phenomena.

Subsequently, following the innovative approach underlying the new Italian Guidelines, an accurate assessment of the beam's residual capacity was performed by comparing it with the maximum expected stresses, in order to determine the potential need for a static rehabilitation intervention. As for the proposed intervention, the key aspects influencing its design and, consequently, its effectiveness were highlighted.

Thanks to nonlinear finite element simulations, it was possible to conduct a long-term analysis that simultaneously takes into account both the effect of the intervention and the overtime evolution of degradation induced by corrosion. Therefore, the novelty of the proposed approach is to accurately assess the overtime variation of the load-bearing capacity of the beam, even when subjected to an intervention, in order to quantify its long-term effectiveness as well as the whole durability.

2 FINITE ELEMENT ANALYSIS OF THE CASE STUDY BEAM

2.1 *Modelling*

The analysed case study is represented by an edge beam of a highway bridge with a simply supported span system, built in 1966 using prestressed reinforced concrete technology with post-tensioned cables. The bridge deck has an overall length of 32.80 m and a width of 11.05 m, consisting of 5 prestressed reinforced concrete beams with a height of 1.7 m, spaced at a distance of 2.20 m (Figure 1a). The 5 beams are connected at the top by a reinforced concrete slab with a thickness of 20 cm and by 5 reinforced concrete transverse beams. Furthermore, crucial information for the analysis, related to the arrangement of the beam and slab reinforcement, as well as the prestressing cable layout, was derived from the design documents (Figure 1b).

The software used for finite element analysis is ATENA (Červenka et al. 2021), which allows for detailed analysis by constructing three-dimensional models. Additionally, the software accounts for concrete and reinforcement nonlinear behaviour. Specifically, for concrete a constitutive model capable of reproducing its behaviour under both compressive (crushing) and tensile (cracking) loading was utilized (Bazant & Oh 1983). Further details on the constitutive model used can be found in the work conducted by (Santarsiero et al. 2021). As for the reinforcement and prestressing cables, an elastic-plastic hardening constitutive model for steel was employed (Ministry of Infrastructure 2018).

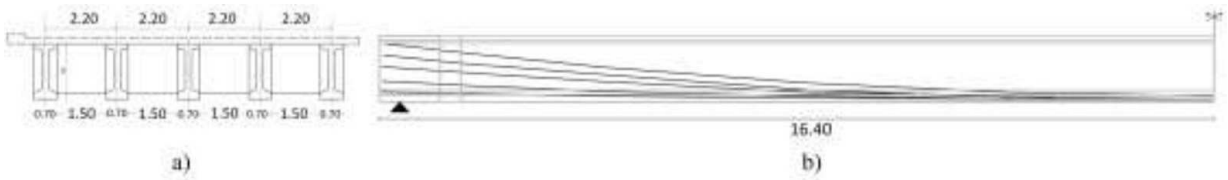

Figure 1. a) Bridge deck's cross-section; b) longitudinal profile of the beam and layout of the post-tensioning cables for half length.

To determine the mechanical properties of reinforcement bars, prestressing cables, and slab concrete, a reference to literature studies was made. However, to estimate the prestressing applied to the cables and the concrete class of the beam, the approach followed was that of "simulated design". This type of approach involves the ability to follow the design phases of the structure, using the regulatory tools of the time, in order to have an understanding of the materials used and construction details, even in the absence of explicit information.

Regarding the reinforcements of the slab and the beam, two types of steel, namely "TOR50" and "AQ50", were used. Given the steel types, it was possible, with the studies of Masi & Digrisolo (2013) and Verderame et al. (2011), to deduce the mean and characteristic values of the parameters necessary for modelling, such as yielding and ultimate tensile strength and strain. In order to conduct safety verifications in accordance with the current regulations (Ministry of Infrastructure 2018), the design strengths used in the software were calculated from these values (Table 1), as specified in the Italian Guidelines (Ministry of Infrastructure, CSLP 2020). In particular, the design values are derived through the following expression:

$$f_d = \min\left(\frac{f_m}{CF \cdot \gamma_m}; \frac{f_k}{CF}\right) \tag{1}$$

where γ_m represents the material safety factor (equal to 1.15 for steel and 1.5 for concrete) (Ministry of Infrastructure 2018), while the term CF represents the confidence factor, which depends on the level of knowledge of the structure (Circolare No. 7/C.S.LL.PP 2019), and has been assumed equal to 1.

As for the prestressing cables, reference was made to the studies by Jacinto et al. (2012) to obtain the characteristic values of strength at 0.1% deformation and rupture ($f_{p0.1k}$ = 1632 MPa, f_{ptk} = 1860 MPa, ε_t = 5%) and, from these, design strengths used within the modelling were derived. Furthermore, in order to model the presence of the protective duct for the prestressing cables (Corven & Moreton 2013), reproducing a certain delay in the onset of cable corrosion during the degrading simulations, the cross-sectional area of each cable has been increased by an amount equal to the cross-sectional area of the duct itself. Therefore, the strength values were reduced to ensure equivalence in terms of force within each cable. Knowing that each cable is made up of 44 strands with a 6 mm diameter and that the duct has a thickness of 0.3 mm, the reduced yield strength values were obtained as $f'_{p0.1d}$ = 1362.54 MPa and ultimate tensile strength as f'_{ptd} = 1552.9 MPa.

Table 2 presents the main strength characteristics of the concrete in the slab and the beam. In the first case, the mean and characteristic strength values were obtained referring to the study by Miluccio et al. (2021). In the second case, the minimum compressive strength value f_{ck} was calculated to ensure that the maximum compressive stress within the beam, subjected to self-weight and cables' prestress, did not exceed the allowable value equal to 48% of the cubic compressive strength, as specified by the regulations in force at the time of design (Circolare No. 384 of 1962). In both cases, once the mean and/or characteristic strength were known, Young's modulus and tensile strength were determined using expressions from the current regulations (Ministry of Infrastructure 2018), while the fracture energy was calculated following the guidelines provided in the Model Code 2010 (Fib, Fédération Internationale du Béton 2010).

Table 1. Strength characteristics of ordinary reinforcement.

	AQ50	TOR50
Young's modulus, E	200 GPa	200 GPa
Design yielding stress, f_{yd}	321.02 MPa	306.55 MPa
Failure stress, f_{td}	475.53 MPa	442.99 MPa
Failure strain, ε_t	0.26 (-)	0.255 (-)

Table 2. Concrete properties for nonlinear simulations.

	Beam	Slab
Design compressive strength, f_{cd}	32 MPa	20.81 MPa
Design tensile strength, f_{td}	2.34 MPa	1.59 MPa
Young's modulus, E	35,220.46 MPa	31,953.76 MPa
Fracture energy, G_F	1.47E−4 MN/m	1.38E−4 MN/m

The assessment of prestressing forces within the cables was carried out by retracing the design phases prescribed by the regulations of that time, in order to achieve a state of integral compressive stress (Leonhardt 1979) within the beam, both when subjected only to self-weight and in operational condition considering permanent and traffic loads (Circolare No. 384 of 1962). In doing so, a value of the prestress applied to the individual cable was obtained, equal to $\sigma_{p,i}$ = 1090 MPa, which is approximately 80% of the cables' yield strength.

Figure 2 shows the 3D finite element model of the analysed beam, discretized into finite elements (3000 hexahedral elements, 49,387 tetrahedral elements, 1824 linear elements, for a total of 22,868 nodes). In particular, taking advantage of the beam's symmetry, only half of it was modelled. Load conditions were applied through a plate located at the midpoint of the beam, while the lower plate transferred the boundary conditions to the model. Both plates were modelled using linear elastic steel behaviour.

The analysis considered the initiation and development of reinforcement and prestressing cable corrosion due to chloride ingress. In fact, the ATENA software allows for mechano-chemical analyses that take into account chloride diffusion inside the concrete, accelerated by the presence of cracking generated by applied loads on the beam. These analyses quantify the time of corrosion initiation and the percentage of corrosion, understood as a reduction in the cross-sectional area, on the reinforcement and prestressing cables. The model was described in detail in Santarsiero et al. (2021) and Santarsiero & Picciano (2023). In particular, by appropriately selecting the values of the main model parameters (surface chlorides concentration C_s, chlorides diffusion coefficient D_{ref}, and critical chlorides content C_{crit}) to consider an aggressive environment due to the use of de-icing salts (Hájková et al. 2018), it was possible to simulate a common degradation condition within bridge beams, where the most deteriorated areas are evident at the locations of water drainage systems and the ends of the beams.

In this way, several analyses were implemented to assess the beam's capacity in as-built conditions and under degraded conditions following time scenarios of 56, 86, and 106 years, which respectively correspond to the current age of the bridge and an additional 30 and 50 years of corrosion development. In each analysis, different intervals can be distinguished as follows: from the first to the fifth interval, the self-weight of the beam and the prestressing force $\sigma_{p,i}$ in each of the 5 prestressing cables are applied; in the sixth interval, the weight of the slab and permanent loads are applied; in the analyses with corrosion simulation, the seventh interval corresponds to the application of the mechano-chemical model; in the final interval, through a displacement-controlled analysis, the beam is brought to failure to assess its ultimate capacity.

Figure 2. Finite element model of the beam.

2.2 *Analyses' results and verifications*

Thanks to the finite element analyses, it was possible to assess the overtime progression of the beam's load-bearing capacity following the considered corrosion scenarios. The beam's capacity was evaluated in terms of flexural strength, resulting in a value of 15,130 kNm in the as-built condition. This capacity undergoes reductions of approximately 10.7% (M_{rd} = 13,520 kNm), 46.5% (M_{rd} = 8100 kNm), and 55.3% (M_{rd} = 6771 kNm), following corrosion development scenarios respectively of 56, 86, and 106 years. As shown in Figure 3, which represents the overtime progression of the maximum corrosion percentage on the prestressing cables, the variations in the beam's strength are justified by a reduction in the cross-sectional area of the cables, ranging from a minimum of 20.5% to a maximum of 36.5% after 56 years, between 30.1% and 67.1% after 86 years, and between 36.2% and 82% following 106 years of corrosion development.

It is worth noting that the mechano-chemical model implemented takes into account the presence of cracks, which increase the possibility of chloride ingress. Furthermore, due to the specific arrangement of the cables within the beam, they are subject to different initiation times, and therefore, the function representing the corrosion progression does not maintain the same concavity throughout the structure's life. This also results in terms of the beam strength variation, showing a nonlinear trend, as demonstrated by the different values of the decay rate obtained in the various time intervals considered. In particular, the first 56 years show a decay of 0.19%, compared to 1.34% between 56 and 86 years, and 0.82% between 86 and 106 years (Figure 4).

Subsequently, to perform the flexural strength verification of the beam, the demand in terms of flexural stress was calculated considering the application of traffic and permanent loads according to the current Italian regulations (Ministry of Infrastructure 2018). Regarding the traffic ones, load pattern No. 1 for global verification includes both tandem concentrated loads Q_{ik} and distributed ones q_{ik}, arranged in 3 conventional lanes with a width of 3 m, as shown in Figure 5. Proceeding with the transverse load distribution procedure by Courbon Engesser (Raithel 1977), a load of 40.62 kN/m on the edge beam is obtained. Using the ultimate limit state combination, this value is combined with structural permanent loads (self-weight of the beam, slab, and concrete curbs) and non-structural permanent loads (pavement and safety devices), resulting in an overall load value on the edge beam of 99.6 kN/m, which produces a maximum midspan flexural demand, for a simply supported beam, of M_{ed} = 13,391.15 kNm.

Figure 4 shows the overtime progression of the ratio between the beam's capacity, assessed through numerical simulations considering the corrosion-induced degradation, and the demand assessed according to current regulations. As can be seen, the flexural verification is satisfied in the as-built condition, with a value of ζ = 1.13, and in the current condition (t = 56 years), although with a very limited safety margin (ζ = 1.01), which leads to exceeding the capacity in subsequent periods (ζ = 0.60 at t = 86 years and ζ = 0.51 at t = 106 years). Therefore, in the next section, the design of a strengthening intervention is carried out.

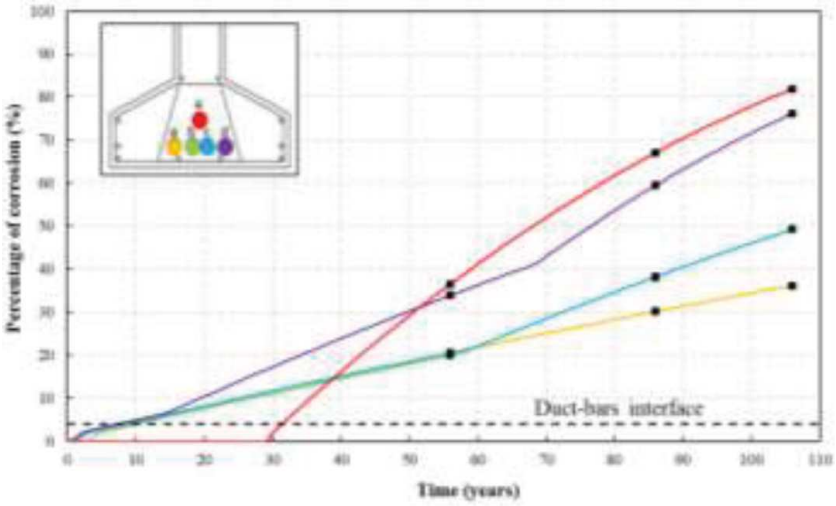

Figure 3. Progression of maximum prestressing cables' corrosion over time.

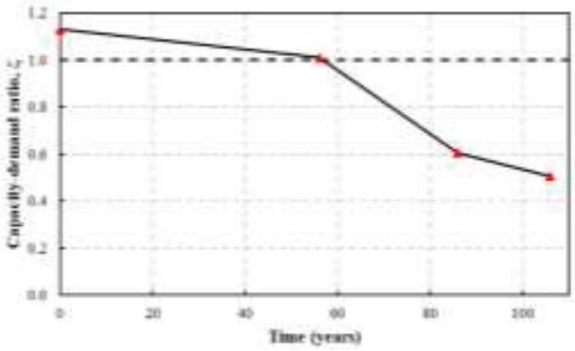

Figure 4. Capacity-demand ratio as a function of time.

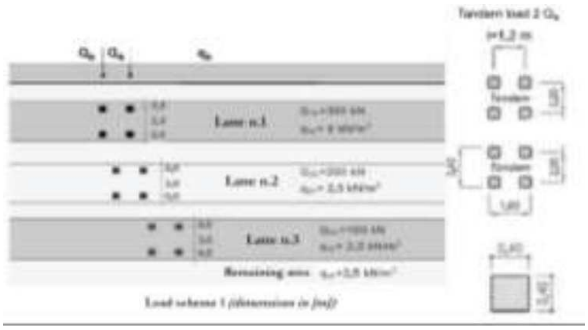

Figure 5. Load pattern No. 1 according to Ministry of Infrastructure (2018).

3 DESIGN AND MODELLING OF EXTERNAL POST-TENSION INTERVENTION

The intervention consists of 2 post-tensioned external cables appropriately arranged along the lateral surfaces of the beam and anchored to it through anchoring plates and deviator plates required for the transfer of the imposed load state. Through cables' tensioning, a compressive force is applied to the structure, increasing its flexural capacity, reducing deflection, and partially or fully recovering existing crack patterns, improving both the serviceability and ultimate limit state performance (Daly & Witarnawan 1997).

In this case, the strengthening system was designed by evaluating the cable prestressing force required to compensate for the deficit in terms of the beam's flexural resistance, as assessed in the previous section. In addition, the assessment of the design prestressing value also depends on the cable's geometry, by evaluating its inclination and eccentricity at the deviator plates. Through iterative steps, the design force of each cable was evaluated equal to T = 1733.13 kN, considering an inclination of 11 degrees and an eccentricity value of 1760 mm. Based on the calculated design force, a cable consisting of 12 strands with a 15 mm diameter was selected from a commercial catalogue, with a yielding strength of $f_{y,e}$ = 1550 MPa, an ultimate tensile strength of $f_{t,e}$ = 1770 MPa, and a failure load of 3180 kN. According to the procedure proposed by MacGregor et al. (1989), the designed cable must also be verified against the increased force to which it would be subjected following a possible failure of the beam, considering a collapse mechanism with the formation of a plastic hinge at midspan. In the end, taking into account this additional verification, a cable prestressing stress of $\sigma_{p,e}$ = 963 MPa was obtained.

Figure 6 shows the 3D model of the beam with the intervention, in which 3 C-plates in S275JR ordinary steel (EN 1993-1-1 2005) have been inserted to anchor the cables at the beam's head and at the locations where they change direction. Therefore, a preliminary nonlinear analysis was implemented to assess the capacity of the reinforced beam, considering that the intervention was applied at t = 56 years, during which the corrosion progression was simulated as seen earlier. Subsequently, two additional scenarios were analysed in which, following the intervention, the beam was subjected to further 30 and 50 years of corrosion development.

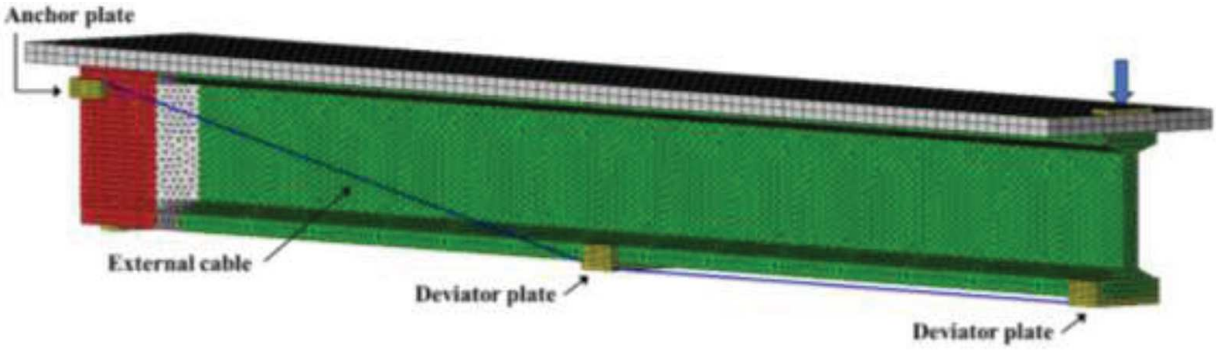

Figure 6. Finite element model of the beam with the intervention.

4 MAIN RESULTS AND DISCUSSION

The implemented nonlinear analyses allowed for the evaluation of the overtime evolution of the beam's capacity-demand ratio, both with and without the strengthening intervention using post-tensioned external cables, as shown in the graph of Figure 7. As can be observed, compared to the conditions without intervention at t = 56 years (current bridge conditions), there is an increase in flexural capacity of approximately 46%, which goes from a value of 13,520 kNm to 19,758 kNm. Additionally, thanks to the intervention, the beam's capacity remains higher than the demand even during the subsequent years of simulated corrosion progression, unlike the case without intervention. In particular, capacity-demand ratio values ζ are 1.48, 1.15, and 1.10, respectively at t = 56, 86, and 106 years with intervention. Another result that can be deduced from the graph is that there is a delayed decrease in strength over time. This is evident from the shallower slope of the lines with the intervention compared to those in as-built corroded conditions in the periods between 56 and 86 years and between 86 and 106 years. In fact, there is an annual decay rate of 0.73% compared to 1.34% without intervention in the first period, while there is a decay of 0.23% compared to 0.82% without intervention in the second one.

Furthermore, the intervention allows for a reduction in the extent of cracking observed at the beam's failure condition. In fact, nonlinear simulations enable the quantification of the maximum crack width, which, in the degraded condition after 56 years of corrosion development, amounts to 2.4 cm (corresponding to reaching a flexural capacity of 13,520 kNm). Conversely, under similar degradation conditions but with the intervention, the maximum crack width is reduced to 1.1 cm (with a flexural capacity of 19,758 kNm), resulting in a 54% reduction. The beneficial effect of external post-tensioning is also evident in terms of beam deformation, reaching a maximum displacement at failure of 16.3 cm, compared to the value of 33.4 cm achieved without intervention and under similar degradation conditions.

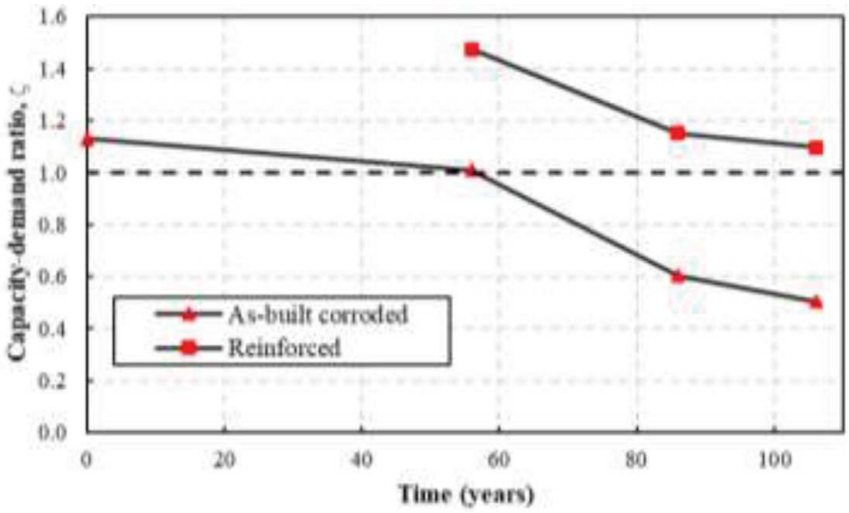

Figure 7. Overtime evolution of capacity-demand ratio in the presence and absence of intervention.

5 CONCLUSIONS

In this study, the structural behaviour of a prestressed reinforced concrete bridge beam built in the 1960s was analysed. The beam was assessed using the finite element software ATENA, which is capable of conducting nonlinear analyses and durability assessments, taking into account chloride-induced corrosion through an advanced mechano-chemical model. The primary objective was to initially evaluate the time-dependent evolution of the structure's capacity under various corrosion scenarios, simulating the current condition of the bridge as well as an additional 30 and 50 years of degradation. Subsequently, this evaluation was compared

to the demand derived from traffic loading patterns in accordance with current Italian regulations. This comparison revealed the need for a strengthening intervention. Therefore, an intervention was designed and modelled, involving the use of external post-tensioned cables. The effectiveness of this intervention was evaluated through a long-term analysis, subjecting the beam to the same corrosion scenarios as before. The results indicate that the intervention increases the flexural capacity of the beam by 46%, raising the capacity-demand ratio from 1.01, in the absence of intervention, to 1.48 in the current state, and maintaining this ratio above 1 even after additional 50 years of degradation. This highlights the effectiveness of the intervention over the long term. Additionally, the beam experiences beneficial effects in terms of cracking and deformation at failure, reducing the maximum crack width and mid-span displacement by 54% and 51%, respectively.

ACKNOWLEDGMENTS

The studies presented here were carried out as part of the activities envisaged by the Agreement between the Italian Department of Civil Protection and the ReLUIS Consortium (DPC-ReLUIS project 2022-24, WP5-Task 5.4 "Upgrading and retrofitting interventions of existing bridges"). The contents of this paper represent the authors' ideas and do not necessarily correspond to the official opinion and policies of DPC.

REFERENCES

Bazant, Z. P., & Oh, B. H. (1983). Crack Band Theory for Fracture of Concrete. *Materials and Structures*, *16*(3), 155–177

Červenka, V., Jendele, L., & Jan Červenka, J. (2021). ATENA Program Documentation, Part 1, *ATENA Theory Manual*, 2000-2021.

Circolare n. 384 del 1962 del Ministero LL.PP. "*Norme relative ai carichi per il calcolo dei ponti stradali*" (Ministero dei Lavori Pubblici). (in Italian).

Circolare n 7.C.S.LL.PP. del 21/01/2019. (2019). *Istruzioni per L'applicazione dell'"Aggiornamento Delle Norme Tecniche per le Costruzioni*" di cui al Decreto Ministeriale 17 Gennaio 2018. (in Italian).

Corven, J., & Moreton, A. J. (2013). *Post-tensioning tendon installation and grouting manual* (No. FHWA-NHI-13-026). Federal Highway Administration (US).

Daly, A. F., & Witarnawan, W. (1997). Strengthening of bridges using external post-tensioning. In *Conference of eastern Asia society for transportation studies* (October 1997), Seoul, Korea.

Di Prisco, M. (2019). Critical infrastructures in Italy: State of the art, case studies, rational approaches to select the intervention priorities. In *fib Symposium 2019: Concrete-Innovations in Materials, Design and Structures* (pp. 49–58). International Federation for Structural Concrete.

EN 1993-1-1 (2005) (English): *Eurocode 3: Design of steel structures - Part 1-1: General rules and rules for buildings* [Authority: The European Union Per Regulation 305/2011, Directive 98/34/EC, Directive 2004/18/EC]

Fib, Federation Internationale du Beton. (2010). *Model Code 2010* First Complete Draft, Fib Bulletin n. 55, vol. 1, Lausanne, Switzerland, 2010

Gjørv, O. E. (2009). *Durability Design of Concrete Structures in Severe Environments*. Taylor & Francis: London, UK; New York, NY, USA.

Godart, B. (2015). Pathology, appraisal, repair and management of old prestressed concrete beam and slab bridges. *Structure and Infrastructure Engineering*, *11*(4), 501–518.

Hájková, K., Šmilauer, V., Jendele, L., & Červenka, J. (2018). Prediction of reinforcement corrosion due to chloride ingress and its effects on serviceability. *Engineering Structures*, *174*, 768–777.

Jacinto, L., Pipa, M., Neves, L. A., & Santos, L. O. (2012). Probabilistic models for mechanical properties of prestressing strands. Construction and Building Materials, 36, 84–89.

Leonhardt, F. (1979). *C.a. & c.a.p.: calcolo di progetto & tecniche costruttive*. Edizioni di scienza e tecnica.

MacGregor, R.J.G., Kreger, M.E., Breen, J.E. (1989). *Strength and Ductility of a Three-Span Externally Post-Tensioned Segmental Box-Girder Bridge Model*. Research Report 365-3F, Project 3-5-85/8-365, Centre for Transportation Research, Bureau of Engineering Research, The University of Texas at Austin, January.

Masi, A., & Digrisolo, A. (2013). Analisi delle caratteristiche meccaniche di acciai estratti da edifici esistenti in cemento armato. In *Proceedings of the ANIDIS XY Conference" L'Ingegneria Sismica in Italia"*, Padova (Vol. 30).

Miluccio, G., Losanno, D., Parisi, F., & Cosenza, E. (2021). Traffic-load fragility models for prestressed concrete girder decks of existing Italian highway bridges. *Engineering Structures*, *249*, 113367.

Ministry of Infrastructure, CSLP. (2020). *Guidelines on Risk Classification and Management, Safety Assessment and Monitoring of Existing Bridges*. Ministry of Infrastructure: Rome, Italy, 2020 (in Italian).

Ministry of Infrastructure. (2018). *Aggiornamento delle Norme tecniche per le costruzioni*. Ministry of Infrastructure, DM 17 Gennaio 2018, Suppl. or. n.30 alla G.U. n.29 del 4/2/2008. (in Italian).

Raithel, A. (1977). *Costruzioni di ponti*. Napoli (in Italian).

Santarsiero, G., & Picciano, V. (2023). Durability enhancement of half-joints in RC bridges through external prestressed tendons: The Musmeci Bridge's case study. *Case Studies in Construction Materials*, *18*, e01813.

Santarsiero, G., Albanese, P., Picciano, V., Ventura, G., & Masi, A. (2023). Level 3 Assessment of Highway Girder Deck Bridges according to the Italian Guidelines: Influence of Transverse Load Distribution. *Buildings*, *13*(7), 1836.

Santarsiero, G., Masi, A., & Picciano, V. (2021). Durability of Gerber saddles in RC bridges: Analyses and applications (Musmeci Bridge, Italy). *Infrastructures*, *6*(2), 25.

Smith, L. J., & Wood, R. (2001). Grouting of external tendons-a practical perspective. *Proceedings of the Institution of Civil Engineers-Structures and Buildings*, *146*(1), 93–100.

Verderame, G. M., Ricci, P., Esposito, M., & Sansiviero, F. C. (2011). Le caratteristiche meccaniche degli acciai impiegati nelle strutture in ca realizzate dal 1950 al 1980. *XXVI Convegno Nazionale AICAP*.